#11508

NUMERICAL STUDY OF PERSONAL EXPOSURE TO CONTAMINANT AND DRAFT RISK IN A WORKSHOP WITH DISPLACEMENT VENTILATION

Shia-Hui Peng[1,2] AND Lars Davidson[2]

[1] Dept. of Work Organization and Technology, National Institute for Working Life, S-171 84 Solna, Sweden
[2] Dept. of Thermo and Fluid Dynamics, Chalmers University of Technology, S-412 96 Gothenburg, Sweden

ABSTRACT

Contaminant dispersion and potential draft risk in a workshop with displacement ventilation were investigated with computational fluid dynamics (CFD) techniques. Three factors were considered: the location of the worker, the temperature of the supply air and the supply air flow rate. The capacity of CFD is demonstrated in optimizing the operation of a ventilation system by weighting two significant aspects, i.e., the indoor air quality and the worker's thermal sensation. On the basis of the numerical results, some suggestions are given for a better use of displacement ventilation systems.

KEYWORDS

displacement ventilation; *breathing-zone concentration*; *draft risk*; *numerical method*

INTRODUCTION

Displacement ventilation has been proven to be an efficient approach in removing indoor contaminants and/or excess heat. The basic principle of this ventilation system is two-fold: cooled, fresh air is supplied on floor level at a low momentum; upwards buoyant convections created by indoor heat sources then bring the air in the lower zone into the upper zone where the contaminated air and/or excess heat are exhausted. The buoyancy thus becomes the virtual origin to make a displacement ventilation flow system function well. The mechanism of inducing buoyancy relies strongly on the behaviour of both air supply and heat source. To understand the performance of this system, special attention must be paid to air diffusion and buoyant convection and their interaction (Peng, 1991; 1993). Intensive studies on this ventilation system have been made in both experiments and with CFD techniques, see e.g. Jacobson (1993), Nielsen (1993) and Mundt (1996).

As with traditional mixing ventilation, displacement ventilation has its pros and cons. One of the drawbacks encountered in applications is concerned with potential thermal discomfort caused by vertical thermal stratification, which is a natural outcome of the aforementioned buoyancy-induced air motion. Moreover, a general concept in displacement ventilation flow is that a stratification front is formed between the lower and upper zones at which the upwards convective air flow rate is equal to the supplied air flow rate. Further, the air motion in the lower zone is often regarded as being of a piston-like type. In practice, the system design has actually benefited from this idea to determine the air exchange corresponding to a required stratification height. The real flow created by a displacement ventilation system, however, is much more complicated. The air motion (plume) above a heat source is normally upwards and piston-like, but the flow surrounding the plume is often of mixing and recirculating air motion owing to entrainment. Such an air flow cannot ensure that the contaminated air is fully upwards-directed into the upper zone and exhausted. By contrast, the contaminant could be dispersed into the worker's breathing zone as a result of recirculating air motion, depending on the relative positions of the worker, the pollutant source, and the heat source.

By means of CFD techniques, this

study investigates the worker's exposure to contaminants in the breathing zone and to cold air at foot level in a workshop with displacement ventilation. A simplified manikin is used to simulate a standing worker at four working positions. The effect of air supply conditions is studied. It is demonstrated how numerical experiments can be used for optimizing the performance of a displacement ventilation system to diminish the exposure to contaminant and cold air.

PROBLEM STATEMENT AND METHOD

The workshop has dimensions of 8 m × 3.6 m × 6 m in the *x*- *y*- and *z*-directions, respectively, see Fig. 1. Material processing is carried out on a working platform (1.8 m × 0.8 m × 1.2 m). The air diffuser (with a surface area of 0.6 m × 0.8 m) is located on a side wall. A convective heating panel (1.2 m × 0.6 m) is mounted on the opposite wall, releasing heat at a constant rate of 1.7 kW. Also located on the opposite wall is the outlet (0.6 m × 0.3 m) below the ceiling. The back wall is towards the outdoors, losing 0.4 kW of heat in winter time. The other enclosures are assumed to be adiabatic. Two fluorescent lamps of 60 W are hung 0.5 m above the centre of the platform, which has the same centreline as do the inlet, the outlet and the heating panel.

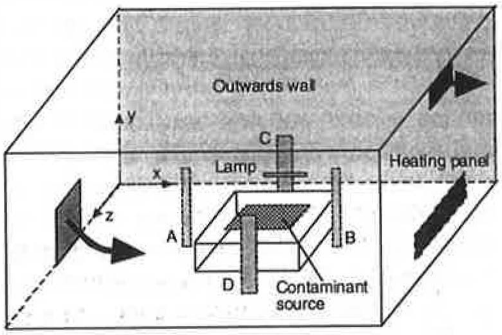

Fig. 1 Configuration of the workshop.

The worker is simulated using a simple geometry with dimensions of 1.7 m × 0.4 m × 0.2 m. This gives an exposed surface area of 2.12 m^2. The heat released from the manikin is 50 W/m^2, corresponding to a moderate activity level for a standing person (about 2 met). During the procedure of material processing, passive contaminants are released at a rate of 10 mg/s over an area of 1.0 m × 0.5 m on the platform surface. The worker may operate at the four sides of the platform (positions A, B , C and D as shown in Fig. 1). One of the objectives of this work is to find which position gives the lowest risk to the worker exposed to the contaminant in the breathing zone and to the cold air spreading above the floor.

To numerically simulate a ventilation flow, it is often safe to assume that the flow exhibits chaotic characteristics known as turbulence. This then requires an appropriate turbulence model to correctly reflect the flow physics. It has been reported that a low-Reynolds number (LRN) k-ε model usually returns an unrealistic laminar solution when used for simulating displacement ventilation flows (Davidson, 1989). It is worth mentioning that a k-ω-type model may be an alternative for overcoming this problem, because this model possesses a solution for the specific dissipation rate, ω, as the flow is laminar (k = 0). A recently developed LRN k-ω model (Peng *et al.*, 1997) was applied to the present flow and gave good turbulent solutions. The problem of using an LRN model is that the computation becomes too expensive owing to near-wall resolution with refined grid. This is particularly not preferable in numerical experiments in which a number of simulations often need to be performed. The standard two-equation models were thus used in conjunction with wall functions. In addition to the k-ε model, a high-Re k-ω model (Peng *et al.*, 1996) was also applied. Very little difference was found between the two. Applying the standard k-ε model (Launder and Spalding, 1974) to displacement ventilation flows, Davidson (1989) reported reasonable simulations in previous work. This model is thus used in the present work.

The study is first aimed at finding the working position in which a standing worker suffers minimum exposure to both contaminant and cold air, when the fresh air is supplied at a temperature of T_{in} = 20 °C at three supply velocities of U_{in} = 0.15, 0.3 and 0.5 m/s. The corresponding air changes per hour (ACH) are then ACH = 1.5, 3 and 5, respectively. When the manikin is located in each of the four positions (see Fig. 1), the contaminant concentration in the manikin's breathing zone (C_b), the draft risk at foot level (PD) (Fanger *et al.*, 1988) and the temperature difference between the foot and neck levels (0.1 m and 1.4 m above the floor, respectively) (ΔT_{fn}) were evaluated. The indices are also estimated with no manikin in these positions to reveal the manikin's influence. The concentration in the breathing zone is taken as the averaged value at a height of 1.45 ~ 1.55 m and a distance of 0.05 m from the exposed surface of the manikin to the platform. The PD value is estimated from the maxims of the averaged PD values for four exposed surfaces at the level of 0.1 m above the floor. The temperature difference, ΔT_{fn}, is evaluated by computing the averaged difference near the manikin between the two heights of 0.1 m and 1.4 m above floor.

Through comparison of the results obtained in the above procedure, both the working position and the necessary supply air flow rate can be determined. Based on this determination, the influence of the supply air temperature is then investigated by evaluating the values of C_b, PD and ΔT_{fn} as the supply air temperature is set at T_{in} = 16 °C and 18 °C, respectively. The influence of the heating panel on the flow pattern is also analyzed and discussed.

RESULTS AND DISCUSSION

The air flow when using various ACHs at T_{in} = 20 °C is first studied. The heat sources, including the manikin, the lamp and the heating panel, produce upwards buoyant flows, and a downwards convection is induced over the outer wall owing to heat loss. The spreading of the cold air strongly relies on the supply air flow rate, as T_{in} is fixed. It was found that, when ACH = 1.5, the supply air starts to sink immediately after the supply opening, and largely diffuses over the floor surface, because the vertical buoyancy is dominant over the horizontal momentum (i.e. a large Archimedes number, Ar). With increasing ACH, the near-inlet fresh air diffuses in a more narrow range, and the air flow falls down at a longer distance from the opening. A further increase in ACH will have the air diffused under bias towards the front wall (opposite the outer wall). At ACH = 5, the inflow air hardly diffuses on the outer-wall side. Instead, it impinges on the working platform and then turns perpendicularly towards the outer wall. This flow feature is caused by the downwards convection along the outer wall, which falls down and enhances the outer-wall-side pressure level in the lower zone. Consequently, the spreading of the air to this side is suppressed. It was noticed that increasing ACH will intensify the downwards flow along the outer wall because the upwards buoyant flows induced by heat sources, particularly by the heating panel, entrain more air arising and diffuse it in the near-ceiling upper zone, where the convection along the outer wall attracts more air to fall into the lower zone.

Moreover, it was found that, with all three ACHs used here, most of the contaminant on the platform rises following the buoyant convection created by the lamp. These contaminants, however, are hardly able to reach to the ceiling level, where the flow is generally horizontal and significantly affected by the thermal wall-jet rising above the heating panel. Instead, the contaminant in the upper zone is further convected and diffused. Owing to recirculation and mixing, the contaminated air may be re-dispersed into the lower zone. The interaction between the inflow and the buoyant convections created by heat sources/sinks is essential for the convective heat and contaminant transfer.

The indices, C_b, PD and ΔT_{fn}, predicted under different supply conditions are compared in Tables 1-3, respectively. In Table 1,

C_b is normalized with the concentration in the exhaust opening, C_R, i.e. $C_{bn} = C_b/C_R$. In general, the values of C_{bn} and PD do not show monotonic change with increasing ACH. The temperature difference, ΔT_{fn}, however, decreases with increasing ACH at each position. In practice, ΔT_{fn} is required to be less than 3 °C for thermal comfort, and this is satisfied when using either ACH = 3 or ACH = 5, in which cases the concentrations in the breathing zone are also relatively low at position A. The predicted PD values, however, are too high at position A, which is close the supply opening. Position B generally has the lowest PD value, because the inflow is obstructed by the platform and the mean air velocity there becomes rather small.

Table 1 Predicted $C_{bn} = C_b/C_R$ (T_{in} = 20 °C).

C_{bn}:	with manikin/***with no manikin***		
ACH =	1.5	3.0	5.0
Pos. A	1.75/***2.03***	0.81/***1.98***	0.90/***1.18***
Pos. B	1.15/***1.85***	0.98/***2.11***	1.51/***3.53***
Pos. C	1.73/***2.05***	3.28/***2.46***	1.85/***1.96***
Pos. D	1.37/***1.77***	1.16/***2.25***	1.63/***1.12***

Table 2 Predicted PD (%) (T_{in} = 20 °C).

PD (%):	with manikin/***with no manikin***		
ACH =	1.5	3.0	5.0
Pos. A	6.1/***3.4***	19.4/***21.3***	30.0/***23.6***
Pos. B	2.4/***0.0***	5.0/***0.0***	7.7/***3.3***
Pos. C	7.2/***5.7***	14.7/***12.7***	8.7/***0.3***
Pos. D	7.4/***5.9***	12.3/***12.2***	10.5/***13.0***

Table 3 Predicted ΔT_{fn} (°C) (T_{in} = 20 °C).

ΔT_{fn} (°C):	with manikin/***with no manikin***		
ACH =	1.5	3.0	5.0
Pos. A	4.4/***5.0***	1.8/***2.1***	0.9/***1.4***
Pos. B	3.9/***4.2***	1.5/***1.6***	0.8/***1.0***
Pos. C	4.0/***4.7***	1.9/***2.0***	1.0/***1.2***
Pos. D	4.0/***4.6***	1.5/***1.7***	1.1/***0.9***

When ACH = 5, the inflow retains a high momentum as it reaches the platform, so high that the contaminant above the platform surface is pushed to the exposed face of the manikin standing at position B, thus entailing a large C_{bn} as shown in Table 1. The convection along the outer wall biases the supplied air in the lower zone towards position D at large ACH. In the upper zone, the air flow is mainly horizontal and suppresses the contaminant plume arising with the lamp-induced buoyant convection. The contaminant is then forced to be dispersed to side positions C and D, where high concentrations are detected. Because less fresh air has been diffused to position C, the concentration is particularly high there. At position A, C_{bn} is slightly increased as the ACH increases from 3 to 5. It was found that, at a large ACH, there is a vortex produced in the lower part in front of the manikin at Position A. This vortex is able to introduce contaminants into the breathing zone when the ACH is further increased to, e.g., ACH = 5. In addition, the comparison shows that the result varies in cases with and without account taken for the manikin, particularly for the breathing-zone concentration, which in general becomes smaller as the manikin is simulated because the upwards convection created by the manikin itself brings more or less fresh air at the floor level into the breathing zone. The effect of a manikin on the concentration prediction was also reported by Brohus (1997).

The comparison in Tables 1-3 shows that, to risk less exposure to the contaminant, position A is the best working location, whereas the draft risk is the largest. At position B, the PD value is less related to the supply air flow rate, and the concentration in the breathing zone appears to be acceptable at ACH = 3. Position B is therefore used for further investigating the effect of supply air temperature when ACH = 3.

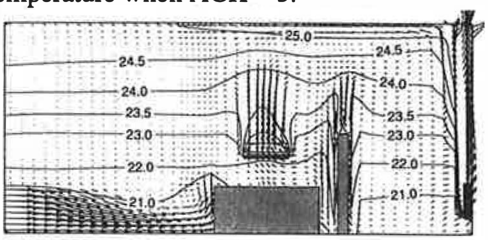

a) Velocity field and T contour, z = 2.95 m.

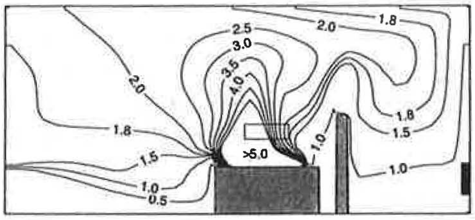

b) C_{bn} contour, $z = 2.95$ m.

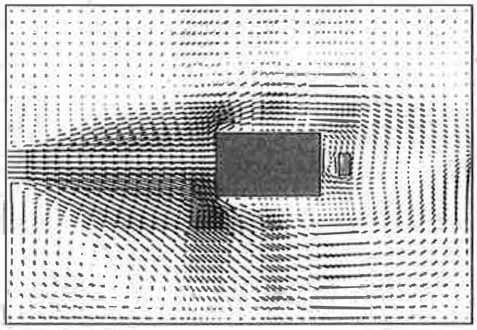

c) Velocity field, $y = 0.15$ m.

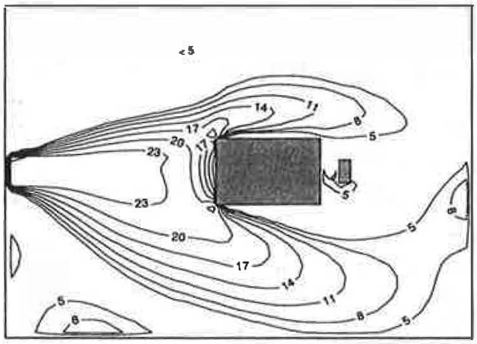

d) PD (%) contour, $y = 0.15$ m.

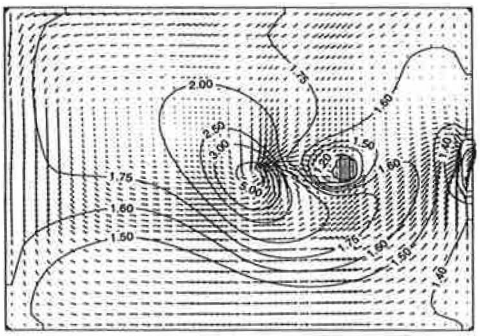

e) Velocity field and C_{bn} contour, $y = 1.55$ m.

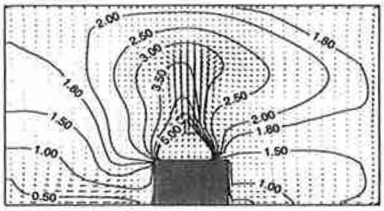

f) Velocity field and C_{bn} contour, $x = 4.45$ m.

Fig. 2 Velocity field and contours of temperature, concentration and PD on various sections with the heating panel installed on the side wall (manikin at position B, ACH = 3 and $T_{in} = 20$ °C).

To gain a straightforward understanding of the flow features, Fig. 2 shows the velocity field and the contours for temperature and concentration on various cross sections when the manikin is placed at position B and the supply conditions are ACH = 3 and $T_{in} = 20$ °C. Also shown in this figure is the PD contour at $y = 0.15$ m above the floor.

As analyzed above, Fig. 2 illustrates that the thermal wall-jet produced by the convective heating panel has played a negative role in decreasing the concentration in the occupied zone. This thermal flow, on the one hand, brings less contaminated air from the floor level into the upper zone; on the other hand, it reinforces the downward convection along the outer wall and helps to transfer contaminants from the upper zone into the lower zone. This thus entails a higher concentration in the region near the outer wall than is found near the opposite wall, see Fig. 2 *e*) and *f*).

Without changing the geometric configuration and the arrangement in the workshop, the effect of the supply air temperature is then investigated when the manikin is placed at position B and ACH = 3. Besides $T_{in} = 20$ °C used above, another two supply air temperatures, $T_{in} = 16$ and 18 °C are specified to observe the change in indices C_{bn}, PD and ΔT_{fn}.

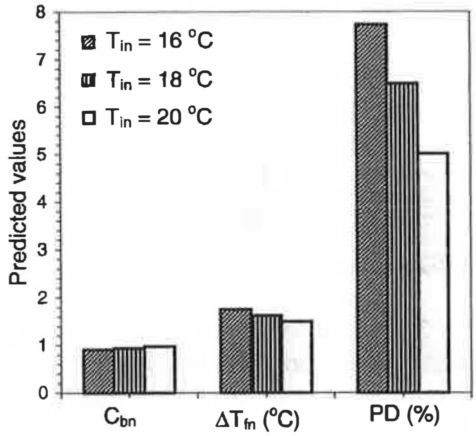

Fig. 3 Predicted indices with various T_{in}'s (manikin at position B, ACH = 3).

Figure 3 shows that the supply air temperature has relatively slight effects on the indices. Decreasing T_{in} from 20 °C to 16 °C, the breathing-zone concentration, C_{bn}, decreases by about 8% at position B, while both ΔT_{fn} and PD increase by about 17% and 54%, respectively, but hold acceptable values. It was found that, at a certain ACH, the flow pattern is only slightly altered with the supply air temperatures used here. The vertical temperature gradient is generally linear. When the location and the strength of the heat sources are kept as in Fig. 1 and ACH = 3, the temperature difference is about 4-5 °C between the ceiling level and the floor level (except in regions where the thermal wall-jet created by the heating panel directly interferes) whichever T_{in} is used. Caution must then be taken for an acceptable thermal environment since too low a T_{in} will decrease the air temperature and induce an overall cold sensation in the occupied zone. To decrease the exposures to both contaminant and cold air, the efficient solution is to optimize the supply air flow and to control the buoyant convections created by heat sources/sinks.

As pointed out above, the outer wall and the heating panel produce undesired convections. The former disperses contaminants into the lower zone, while the latter reinforces such dispersions and brings part of fresh air at floor level directly into the upper zone without sufficiently mixing with the contaminant. To eliminate this problem, this convective heating panel is moved from the side wall and re-mounted on the centre of the outer wall at the same height above the floor as when it was installed on the side wall. It is expected that the upward convection brought about by the heating panel will obstruct the downward buoyant flow along the outer wall so that the contaminant dispersed into the lower zone can be diminished along this wall.

Figure 4 compares indices C_{bn}, PD and ΔT_{fn} when the manikin is placed at position B and the heating panel is installed on two different walls. In both cases, the supply conditions are ACH = 3 and T_{in} = 20 °C. This comparison shows that the concentration in the manikin's breathing zone is apparently decreased when the heating panel is moved from the side wall to the outer wall. The other two indices are also affected. The PD value slightly decreases about 1%. The temperature difference, ΔT_{fn}, increases but holds to be less than 3 °C.

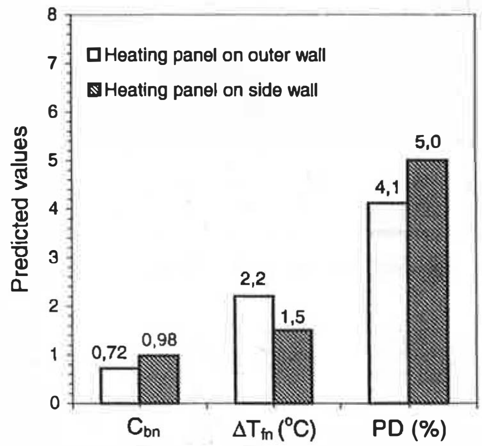

Fig. 4 Predicted indices when the heating panel is installed on different walls (manikin at position B, ACH = 3 and T_{in} = 20 °C).

When the convective heating panel is mounted on the outer wall, the resultant flow features are illustrated in Fig. 5. The thermal wall jet created by the heating panel goes up along the outer wall and significantly diminishes the cold air convection, see e.g. Fig. 5 *f*). The diffusion of the fresh air on the outer wall side is not suppressed in this case. Instead, the entrainment of the thermal wall-jet slightly enhances this diffusion, see Fig. 5 *c*). The vertical temperature gradient, as shown in Fig. 5 *a*), becomes larger than that shown in Fig. 2 *a*). In the region around position B, the contaminant concentration has been efficiently diluted in the lower zone, see Fig. 5 *b*) and *f*). It should be noted that the condition at position A may be deteriorated because of the eddy formed as the sinking inflow approaches the working platform, as shown in Fig. 2 *a*) and Fig. 5 *a*). This eddy tends to attract contaminants from the platform surface to position A.

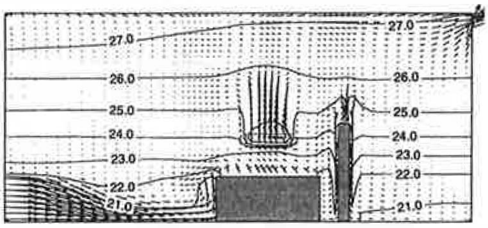

a) Velocity field and T contour, $z = 2.95$ m.

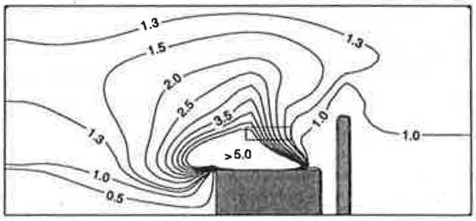

b) C_{bn} contour, $z = 2.95$ m.

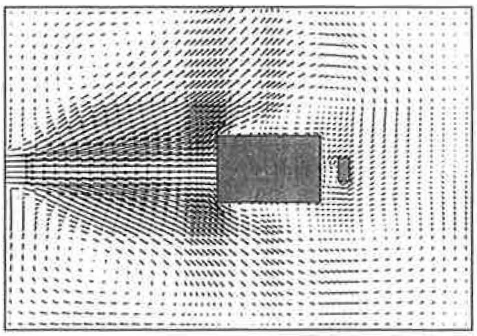

c) Velocity field, $y = 0.15$ m.

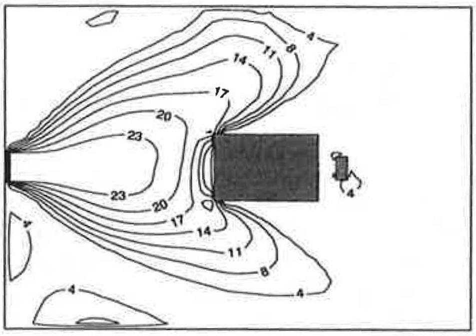

d) PD (%) contour, $y = 0.15$ m.

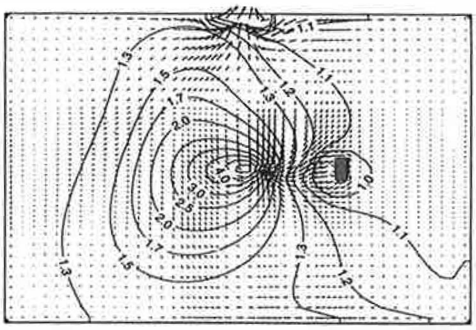

e) Velocity field and C_{bn} contour, $y = 1.55$ m.

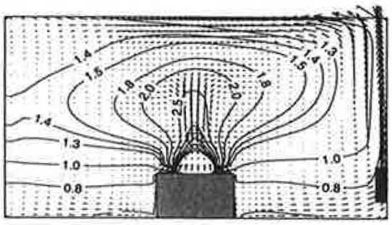

f) Velocity field and C_{bn} contour, $x = 4.45$ m.

Fig. 5 Velocity field and contours for temperature, concentration and PD with the heating panel installed on the outer wall (manikin at position B, ACH = 3 and T_{in} = 20 ^oC).

CONCLUSIONS

The air flow in a workshop with displacement ventilation was studied by means of CFD techniques. The personal exposures to contaminants in the breathing zone and to cold air at foot level were investigated. The use of CFD simulations as a tool to optimize ventilation performance is demonstrated.

It is emphasized that the interaction

between the supply air flow and the buoyant convections created by heat sources/sinks is an essential ingredient in an effective displacement ventilation system that can remove pollutants and heat excess efficiently. In general, as the air supply temperature is changed within an acceptable range, e.g. from 16 °C to 20 °C, the flow pattern is only slightly affected. A small air supply temperature could slightly decrease the breathing-zone concentration, but cause potential cold thermal sensation. To minimize the exposure to the contaminant, the air exchange can be increased. Caution must be taken to choose the correct working position, however, since increasing the ACH by no means decreases the exposure everywhere in the lower zone. Moreover, too high an ACH could increase the foot-level draft risk at some positions, particularly near the supply opening.

It was found that the vertical temperature gradient increases with decreasing ACH. The sink and diffusion of the fresh air after the supply opening depend on the Archimedes number, Ar. A small Ar number makes the supplied air slowly sink and diffuse less to both sides. The heat-losing enclosure induces a downward convection flow, which disperses contaminants from the upper zone into the lower zone. If the other heat sources are misplaced, this downward flow could be reinforced and give rise to a higher lower-zone contaminant concentration. As is often seen in practice, an efficient strategy is to install a heating panel on the heat-losing wall, which produces an upward convection flow, thus impeding the contaminants from being transported downward.

REFERENCES

Brohus, H. (1997) CFD simulation of personal exposure to contaminant sources in ventilated rooms. *Proceedings of Ventilation* '97, Vol. 1, 215-226, Ottawa, Canada.

Davidson, L. (1989) Ventilation by displacement in a three-dimensional room - A numerical study. *Building and Environment*, **24**, 363-372.

Fanger, P. O., Melikov, A. K, Hanzawa, H. and Ring, J. (1988) Air turbulence and sensation of draught, *Energy and Buildings*, **12**, 21-39.

Jacobsen, T. V. (1993) *Airflow and Temperature Distribution in Room with Displacement Ventilation*. Ph. D. Thesis, Aalborg University, Aalborg, Denmark.

Launder, B. E. and Spalding, D. B., (1974) The numerical computation of turbulent flows. *Computer Methods in Applied Mechanics and Engineering*, **3**, 269-189.

Mundt, E. (1996) *The Performance of Displacement Ventilation Systems: Experimental and Theoretical Studies*. Ph. D. Thesis, Royal Institute of Technology, Stockholm, Sweden.

Nielsen, P. V. (1993) *Displacement Ventilation: Theory and Design*. Aalborg University, Aalborg, Denmark.

Peng, S-H. (1991) Displacement ventilation: A primary review. *Report*, Department of Heating and Ventilation, Royal Institute of Technology, Stockholm, Sweden.

Peng, S-H. (1993) Displacement ventilation: A case study. *Report*, Department of Heating and Ventilation, Royal Institute of Technology, Stockholm, Sweden

Peng, S-H., Davidson, L. and Holmberg, S. (1996) The two-equation k-ω turbulence model applied to recirculating ventilation flows, *Report* 96/13, Department of Thermo and Fluid Dynamics, Chalmers University of Technology, Gothenburg, Sweden.

Peng, S-H., Davidson, L. and Holmberg, S. (1997) A modified low-Reynolds-number k-ω model for recirculating flows, ASME *Journal of Fluid Engineering*, **119**, 867-875.